

Replacing the Promoter of the Murine Gene Encoding P-selectin with the Human Promoter Confers Human-like Basal and Inducible Expression in Mice*

Received for publication, November 2, 2015, and in revised form, November 25, 2015 Published, JBC Papers in Press, December 2, 2015, DOI 10.1074/jbc.M115.702126

Zhenghui Liu^{†1}, Nan Zhang^{§1}, Bojing Shao[‡], Sumith R. Panicker[‡], Jianxin Fu[‡], and Rodger P. McEver^{†§2}

From the [‡]Cardiovascular Biology Research Program, Oklahoma Medical Research Foundation, Oklahoma City, Oklahoma 73104 and the [§]Department of Biochemistry and Molecular Biology, University of Oklahoma Health Sciences Center, Oklahoma City, Oklahoma 73104

In humans and mice, megakaryocytes/platelets and endothelial cells constitutively synthesize P-selectin and mobilize it to the plasma membrane to mediate leukocyte rolling during inflammation. TNF- α , interleukin 1 β , and LPS markedly increase P-selectin mRNA in mice but decrease P-selectin mRNA in humans. Transgenic mice bearing the entire human *SELP* gene recapitulate basal and inducible expression of human P-selectin and reveal human-specific differences in P-selectin function. Differences in the human *SELP* and murine *Selp* promoters account for divergent expression *in vitro*, but their significance *in vivo* is not known. Here we generated knockin mice that replace the 1.4-kb proximal *Selp* promoter with the corresponding *SELP* sequence (*Selp*^{KI}). *Selp*^{KI/KI} mice constitutively expressed more P-selectin on platelets and more P-selectin mRNA in tissues but only slightly increased P-selectin mRNA after injection of TNF- α or LPS. Consistent with higher basal expression, leukocytes rolled more slowly on P-selectin in trauma-stimulated venules of *Selp*^{KI/KI} mice. However, TNF- α did not further reduce P-selectin-dependent rolling velocities. Blunted up-regulation of P-selectin mRNA during contact hypersensitivity reduced P-selectin-dependent inflammation in *Selp*^{KI/-} mice. Higher basal P-selectin in *Selp*^{KI/KI} mice compensated for this defect. Therefore, divergent sequences in a short promoter mediate most of the functionally significant differences in expression of human and murine P-selectin *in vivo*.

Neutrophils roll on P- and E-selectin expressed on venular endothelial cells in the first step of the inflammatory response (1–3). Endothelial cells in skin and bone marrow constitutively express E-selectin in humans and mice (4–6). In other tissues, TNF- α , IL-1 β , or LPS translocates NF- κ B, activating transcription factor 2 (ATF-2), and other transcription factors to the nucleus (7). These proteins activate the human *SELE* and murine *Sele* genes by binding to conserved promoter elements.

* This work was supported by National Institutes of Health Grants HL034363 and HL085607. R. P. M. has interests in Selexys and Tetherex. The other authors declare that they have no conflicts of interest with the contents of this article. The content is solely the responsibility of the authors and does not necessarily represent the official views of the National Institutes of Health.

[†] Both authors contributed equally to this work.

[‡] To whom correspondence should be addressed: Cardiovascular Biology Research Program, Oklahoma Medical Research Foundation, 825 N.E. 13th St., Oklahoma City, OK 73104. Tel.: 405-271-6480; Fax: 405-271-3137; E-mail: rodger-mcever@omrf.org.

In humans and mice, megakaryocytes/platelets and endothelial cells constitutively express P-selectin, which is stored in secretory granules (1–3). Resident peritoneal macrophages also express P-selectin (8). Thrombin or histamine rapidly mobilizes the basal stores of P-selectin to the plasma membrane (1–3). TNF- α , IL-1 β , or LPS further up-regulates mRNA for P-selectin in mice (9, 10) and other mammals (11–13) but not in humans and other primates. TNF- α decreases mRNA for P-selectin in cultured human endothelial cells (14–16). Baboons infused with *Escherichia coli* shed LPS and express TNF- α , which increase mRNA for E-selectin but decrease mRNA for P-selectin in many organs (16). Transgenic mice bearing the entire human *SELP* gene constitutively express human P-selectin in megakaryocytes/platelets, endothelial cells, and resident peritoneal macrophages (17). TNF- α or LPS infused into transgenic mice that retain the endogenous *Selp* gene markedly increases mRNA for murine P-selectin but decreases mRNA for human P-selectin in many organs (17). Therefore, the basal and inducible expression of the *SELP* transgene recapitulates that of the native gene in humans.

In vitro studies suggest that distinct elements in the proximal 1.4-kb promoters of the *SELP* and *Selp* genes account, at least in part, for divergent basal and inducible expression of P-selectin in humans and mice. The *Selp* gene has canonical binding sites for NF- κ B (p50/p52 heterodimers) and ATF-2 like those in the *SELE* and *Sele* genes (18). TNF- α increases the expression of a reporter gene driven by the *Selp* promoter in transfected endothelial cells (19). Mutation of the NF- κ B and ATF-2 sites abrogates TNF- α -inducible expression (18). The *SELP* promoter lacks these sites, and TNF- α does not augment the expression of the reporter gene driven by the *SELP* promoter (19). Instead, the *SELP* promoter has a non-canonical binding site for NF- κ B (p50 or p52 homodimers) (20, 21). Mutation of this site reduces constitutive expression of the reporter gene (21). It is not known whether these distinct elements account for the divergent expression of human and murine P-selectin *in vivo*. In this study, we generated knockin mice that replace the 1.4-kb proximal promoter of *Selp* with the corresponding sequence from *SELP*. We compared the basal and inducible expression of murine P-selectin in knockin and WT mice.

Experimental Procedures

Mice—A targeting vector was constructed containing a portion of the murine *Selp* allele (19, 22) in which the 1.4-kb

Human SELP Promoter Function in Mice

sequence immediately before the translation start site was replaced with the corresponding 1.4-kb sequence from the human *SELP* allele (19). A *loxP*-flanked *hygromycin* cassette (a gift from Dr. David S. Milstone, Harvard Medical School, Boston, MA) was inserted into intron 1 for selection of transfected embryonic stem cells with hygromycin B. A thymidine kinase (*tk*) cassette was placed just outside the 3'-flanking homologous sequence to further select targeted clones with ganciclovir. The fidelity of the targeting construct was confirmed by DNA sequencing. The linearized targeting vector was electroporated into C17 murine embryonic stem cells (23). After drug selection, the *loxP*-flanked *hygromycin* cassette was removed by transient *in vitro* expression of Cre recombinase. Targeted clones were confirmed by Southern blot (17). After confirming a normal karyotype, embryonic stem cells from one of the targeted clones were injected into C57BL/6J blastocysts, and the blastocysts were implanted into pseudopregnant mice. Chimeric offspring were bred with C57BL/6J mice for germline transmission. Progeny homozygous for the knockin allele (*Selp*^{KI/KI}) were backcrossed over 10 generations into the C57BL/6J background. Some mice were bred with *Selp*^{-/-} mice (22) (C57BL/6J background, The Jackson Laboratory) to generate heterozygous *Selp*^{KI/-} mice. C57BL/6J mice were used as WT controls. All mice were housed in a specific pathogen-free facility. All animal protocols were approved by the Institutional Animal Care and Use Committee of the Oklahoma Medical Research Foundation.

Peripheral Blood Counts—Peripheral blood counts were measured with a Hemavet 950 veterinary hematology analyzer (Drew Scientific, Inc.).

Flow Cytometry—Whole blood collected by retro-orbital bleeding from anesthetized mice was transferred directly into a tube coated with EDTA (Microvette® 200 potassium EDTA). To study platelets, 2 μ l of blood was diluted 1:100 in Hanks' balanced salt solution (HBSS)³ containing 5 mM EDTA (HBSS/EDTA). In some experiments, diluted blood was incubated with 1 unit/ml human thrombin (EMD Millipore) for 15 min at 37 °C to activate platelets. Resident peritoneal cells were collected by flushing the peritoneal cavity with 6 ml of HBSS/EDTA. All antibody incubations were performed on ice. Cells were preincubated with 5 μ g/ml murine Fc Block (anti-murine CD16/CD32, BD Biosciences) for 15 min. Cells were then incubated for 30 min with 10 μ g/ml of FITC-labeled RB40.34 (rat IgG1, anti-murine P-selectin, BD Biosciences), phycoerythrin-labeled MWReg30 (rat IgG1, anti-murine CD41, BioLegend), phycoerythrin-labeled BM8 (rat IgG2a, anti-murine F4/80, macrophage marker, BioLegend), FITC-labeled 1A8 (rat IgG2a, anti-murine Ly6G, BioLegend), or labeled isotype control mAbs. The cells were then washed, resuspended in HBSS containing 0.1% human serum albumin and 5 mM EDTA, and analyzed on a FACScan instrument using CellQuest software (BD Biosciences). Platelet, macrophage, and neutrophil subpopulations were distinguished by expression of CD41, F4/80, and Ly6G, respectively.

Quantitative RT-PCR (qRT-PCR)—Total RNA from murine lung, heart, liver, and ear was isolated using a RNeasy fibrous tissue mini kit (Qiagen) according to the instructions of the manufacturer. RNA integrity was verified by ethidium bromide staining after electrophoresis and quantified by optical density at 260 nm. 1 μ g of RNA in a 20- μ l reaction volume was reverse-transcribed using SsoAdvancedTM Universal SYBR® Green Supermix (Bio-Rad) as specified by the manufacturer. The RT reaction volume was diluted to 100 μ l with double-distilled H₂O, 2 μ l of which was used as template for qRT-PCR in a 96-well plate with 0.2 μ M of each primer and SYBR® Green PCR Master Mix (Life Technologies). qRT-PCR was performed on a CFX96TM real-time system (Bio-Rad), and amplification was performed according to the protocol of the manufacturer. Relative gene expression was analyzed with CFX ManagerTM software (Bio-Rad) using *gapdh* as an internal control. qRT-PCR assays were conducted in triplicate for each sample. The sequences of *gapdh* primers were 5'-GAAGGTGAAGGT-CGGAGTC-3' (sense) and 5'-GAAGATGGTGATGGGA-TTTC-3' (antisense). The sequences of murine *Selp* primers were 5'-GGTATCCGAAAGATCAACAATAAGTGG-3' (sense) and 5'-TTACTCTTGATGTAGATCTCCACACA-3' (antisense).

Immunofluorescence—Murine tissues were fixed in 4% paraformaldehyde overnight at 4 °C, transferred into 20% sucrose overnight at 4 °C, embedded in Tissue-Tek O.C.T. compound (Triangle Biomedical Sciences, Inc.), and processed into 5- μ m sections. After fixation and permeabilization in acetone at -20 °C for 2 min, cryosections were rinsed with PBS containing 0.01% saponin, incubated with serum-free protein block (Dako) at room temperature for 60 min, and then incubated with goat anti-murine P-selectin polyclonal antibody with 0.01% saponin overnight at 4 °C. The tissue sections were stained with Alexa Fluor 555-conjugated donkey anti-goat IgG antibody with 0.01% saponin at room temperature for 1 h. After washing, mounting medium was added to the slides. The images in the slides were visualized on a Zeiss Axiovert 200 M (Carl Zeiss, LLC) microscope at \times 63 magnification and captured by a Carl Zeiss AxioCam MRm Rev. 3.0 camera using the acquisition software Carl Zeiss AxioVision V. 4.8.

Intravital Microscopy—Intravital video microscopy of anesthetized mice was performed as described previously (17, 23–25). The cremaster muscle was isolated and superfused with thermo-controlled (37 °C) HBSS. Microscopy was performed immediately after isolation or 2 h after intrascrotal injection of murine TNF- α (R&D Systems, 0.5 μ g/mouse in 0.3 ml of sterile saline). A blocking anti-murine E-selectin mAb, 9A9 (26) (30 μ g in 100 μ l of saline), was injected intravenously 3–5 min before TNF- α injection. Microvessel diameters, lengths, and centerline velocities were comparable in mice from all genotypes. Leukocyte rolling velocities were measured as described previously (17, 23–25).

Thioglycollate-induced Peritonitis—Mice were injected intraperitoneally with 1.5 ml of 0.9% saline or 4% thioglycollate. Some mice received 30 μ g of anti-murine P-selectin mAb 5H1 (27) intravenously immediately before administration of thioglycollate. After 4 h, mice were sacrificed, and the peritoneal cavity was lavaged with 6 ml of PBS containing 5 mM EDTA.

³ The abbreviations used are: HBSS, Hanks' balanced salt solution; qRT-PCR, quantitative RT-PCR; KI, knockin.

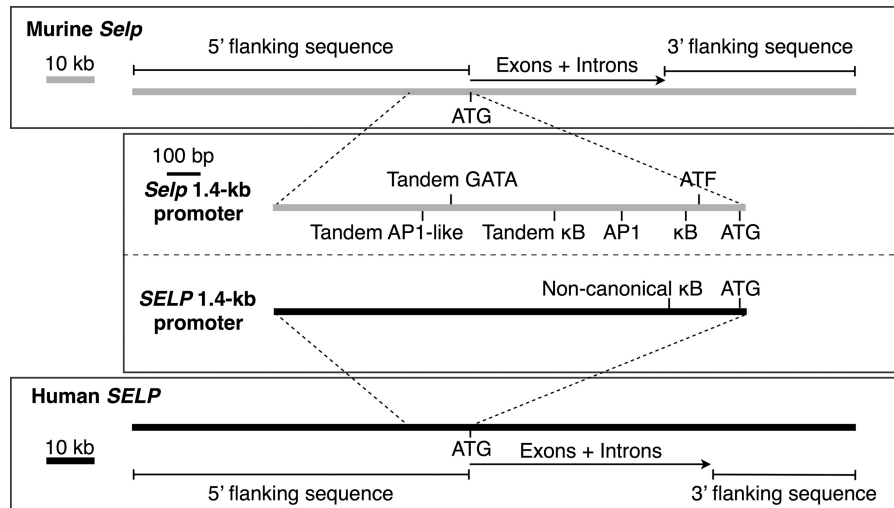


FIGURE 1. **Schematics of the murine *Selp* and human *SELP* genes.** Exon 1 of each gene ends in an ATG codon for the translation start site. Unique elements in the proximal 1.4-kb promoter sequence of each gene are shown. The lengths of the 5' and 3' flanking regions of *SELP* correspond to those incorporated in a *SELP* transgene that recapitulates basal and inducible expression of human P-selectin in mice (17).

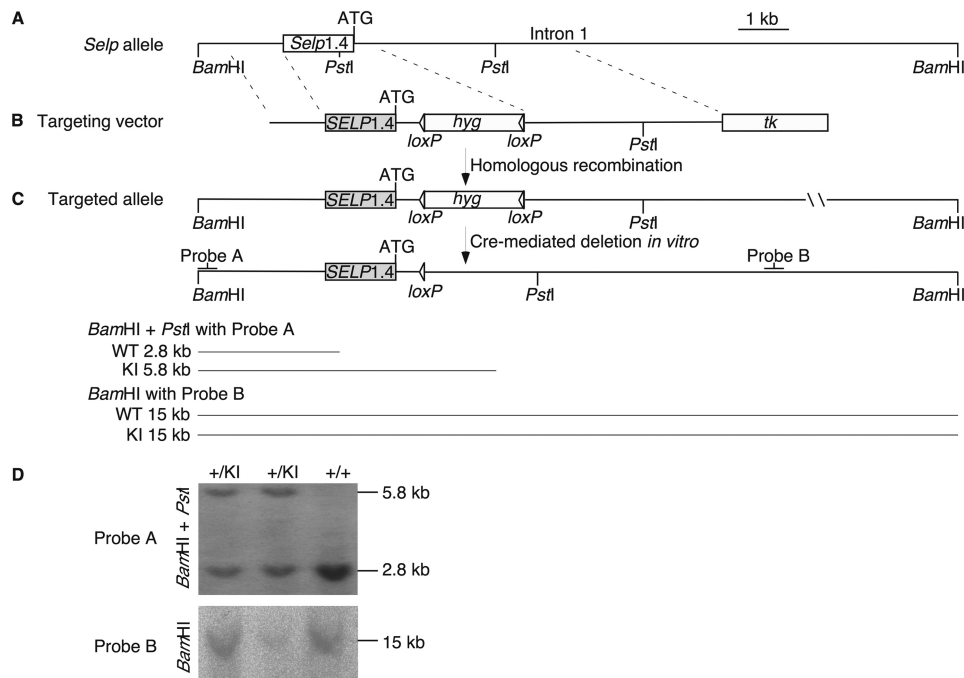


FIGURE 2. **Strategy for generating the *Selp*^{KI} allele.** *A*, partial restriction map of the murine *Selp* allele. *B*, diagram of the targeting vector. *C*, diagram of the targeted (knockin) allele before and after Cre-mediated deletion of the *hygromycin* (*hyg*) selection cassette, the probes used for Southern blots, and the predicted sizes of the restriction fragments for the WT and knockin alleles. *D*, Southern blot of genomic DNA isolated from tails of WT (+/+) mice and of mice expressing one WT and one knockin allele (+/KI).

The recovered cells were analyzed by flow cytometry. Neutrophils were counted on the basis of scatter properties and high expression of Ly6G.

Oxazolone-induced Contact Hypersensitivity—On day 0, mice were sensitized by topical application of 100 μ l of 2% oxazolone (4-ethoxymethylene-2-oxazolin-5-one, Sigma-Aldrich) in acetone/olive oil (4:1) to shaved abdominal skin and of 5 μ l of the same mixture to each paw. On day 7, mice were challenged by painting the right ear with 1% oxazolone (10 μ l on each side). The left ear was painted with acetone/olive oil as a control. In some mice, mAbs (100 μ g in 100 μ l saline) to murine P-selectin (5H1) or murine E-selectin (9A9) were injected intravenously

immediately before the challenge. Control mice were injected with saline. Ear thickness 24 h after challenge was measured with an electronic digital micrometer (Marathon Watch). Ear thickness was expressed as the absolute increase in micrometers and calculated as treated ear thickness – control ear thickness. For flow cytometry, ear tissue collected 24 h after challenge was chopped into small pieces and digested with a mixture containing type I and II collagenase, DNase, and RNase (Roche). After a 3-h digestion at room temperature, the lysate was passed through a 100- μ m strainer and stained with anti-Ly6G and anti-F4/80 antibodies to identify neutrophils and monocyte/macrophages, respectively. To study gene expres-

Human *SELP* Promoter Function in Mice

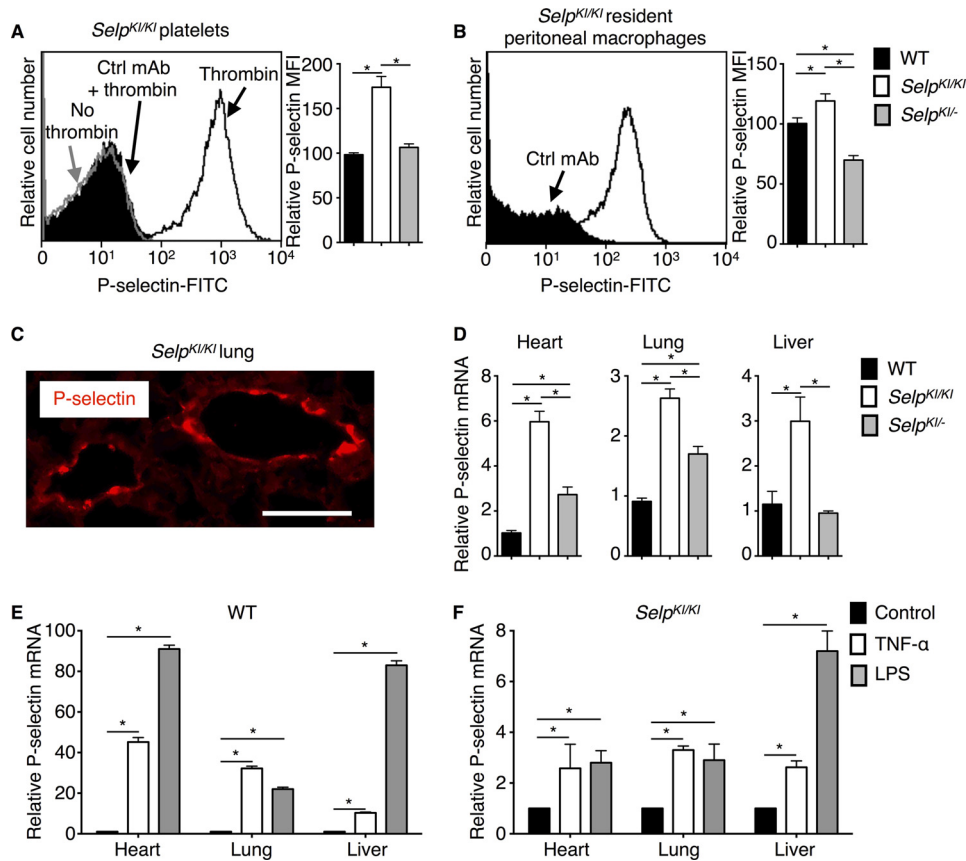


FIGURE 3. Basal and inducible expression of P-selectin in *Selp*^{K1/K1} and *Selp*^{K1/-} mice. *A*, left panel, flow cytometric analysis of resting (no thrombin) or thrombin-activated platelets from *Selp*^{K1/K1} mice stained with FITC-conjugated anti-murine P-selectin mAb or FITC-conjugated control mAb (Ctrl). Right panel, mean fluorescence intensity (MFI) for P-selectin on thrombin-activated platelets from WT, *Selp*^{K1/K1}, or *Selp*^{K1/-} mice ($n = 5-10$ mice/group). *B*, left panel, flow cytometric analysis of resident peritoneal macrophages from *Selp*^{K1/K1} mice stained with FITC-conjugated anti-murine P-selectin mAb or FITC-conjugated control mAb. Right panel, MFI for P-selectin on resident peritoneal macrophages from WT, *Selp*^{K1/K1}, or *Selp*^{K1/-} mice ($n = 5-10$ mice/group). *C*, immunofluorescence of lungs from *Selp*^{K1/K1} mice. Cryosections were incubated with goat anti-P-selectin polyclonal antibody followed by Alexa Fluor 555-conjugated donkey anti-goat antibody and observed under a fluorescence microscope. Red fluorescence indicates the distribution of P-selectin. Scale bar = 50 μm . *D*, total RNA was isolated from tissues of WT, *Selp*^{K1/K1}, or *Selp*^{K1/-} mice. P-selectin mRNA was quantified by real-time PCR. Expression was normalized to mRNA for GAPDH. -Fold changes were normalized to mRNA of WT tissues ($n = 10-15$ mice/group). *E*, quantification of P-selectin mRNA 3 h after intravenous injection of control albumin, TNF- α , or LPS in WT mice normalized to control-treated mice ($n = 10-15$ mice/group). *F*, quantification of P-selectin mRNA 3 h after intravenous injection of control albumin, TNF- α , or LPS in *Selp*^{K1/K1} mice normalized to control-treated mice ($n = 10-15$ mice/group). Error bars are mean \pm S.E. *, $p < 0.05$.

sion, treated and control ears were removed 8 h after challenge, frozen in dry ice, and homogenized in lysis buffer (Qiagen) without thawing. Total RNA was purified using the RNeasy fibrous tissue mini kit (Qiagen). qRT-PCR was performed as described above.

Statistics—Statistical analysis was performed using Student's *t* test for unpaired samples. Results were considered significant at $p < 0.05$.

Results

Human *SELP* and murine *Selp* have similar exon/intron organizations (28, 29) (Fig. 1). A *SELP* transgene encompassing all exons and introns plus 70 kb of 5' flanking sequence and 29 kb of 3' flanking sequence drives the basal and inducible expression of human P-selectin in mice as the native gene does in humans (17) (Fig. 1). *In vitro*, distinct elements in the proximal 1.4-kb promoters of *SELP* and *Selp* mediate species-specific differences in the basal and inducible expression of reporter genes (18–21) (Fig. 1). To determine whether divergence of these short promoters is sufficient to confer species-specific expression *in vivo*, we made knockin mice that replace the

1.4-kb promoter sequence of *Selp* with the corresponding sequence from *SELP* (Fig. 2, A–C). Southern blots of genomic DNA confirmed the correct integration of the targeted allele (Fig. 2D). Some mice homozygous for the knock in allele (*Selp*^{K1/K1}) were bred with *Selp*^{-/-} mice to generate heterozygous *Selp*^{K1/-} mice. Both homozygous and heterozygous knockin mice were healthy with normal blood counts.⁴

Anti-murine P-selectin mAb bound to thrombin-activated but not resting *Selp*^{K1/K1} platelets, consistent with redistribution of P-selectin from α -granules to the plasma membrane (2, 3) (Fig. 3A). Activated *Selp*^{K1/K1} platelets expressed ~1.5-fold more P-selectin than activated WT or *Selp*^{K1/-} platelets. This is consistent with ~1.5-fold higher levels of human P-selectin on activated platelets from homozygous *SELP* transgenic mice than of murine P-selectin on activated platelets from WT mice (17). *Selp*^{K1/K1} peritoneal macrophages also expressed more P-selectin (Fig. 3B). Immunofluorescence revealed staining for P-selectin in venular endothelial cells of the lung (Fig. 3C) and

⁴ Z. Liu, N. Zhang, B. Shao, S. R. Panicker, J. Fu, and R. P. McEver, unpublished data.

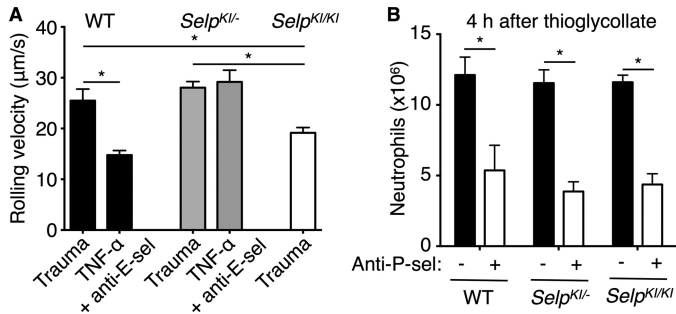


FIGURE 4. P-selectin-dependent neutrophil rolling and migration in *Selp*^{K1/K1} and *Selp*^{K1/-} mice. A, mean leukocyte rolling velocities in trauma-stimulated venules ($n = 150\text{--}200$ leukocytes from 15–20 venules/group) or in TNF- α -stimulated venules of mice injected with blocking anti-E-selectin mAb (*anti-E-sel*) ($n = 320\text{--}330$ leukocytes from 32–33 venules/group). B, WT, *Selp*^{K1/K1}, or *Selp*^{K1/-} mice were injected intraperitoneally with thioglycollate. Some mice were injected intravenously with blocking anti-P-selectin mAb (*anti-P-sel*) at the time of thioglycollate challenge. After 4 h, peritoneal cells were lavaged, and neutrophils were quantified by flow cytometry ($n = 7\text{--}10$ mice/group). *, $p < 0.05$.

other organs.⁴ Basal P-selectin mRNA levels in the heart, lung, and liver were 2- to 6-fold higher in *Selp*^{K1/K1} mice, with intermediate elevations in *Selp*^{K1/-} mice (Fig. 3D). Therefore, *Selp*^{K1/K1} mice express higher basal levels of P-selectin than WT mice. As noted previously (17), WT mice injected intravenously with TNF- α or LPS up-regulated P-selectin mRNA by 10- to 100-fold (Fig. 3E). *Selp*^{K1/K1} mice only up-regulated P-selectin mRNA 2- to 7-fold (Fig. 3F), although the absolute level was greater because of higher basal mRNA expression. TNF- α or LPS decreases P-selectin mRNA in *SELP* transgenic mice (17). Therefore, substituting the *SELP* 1.4-kb promoter sequence eliminates most, but not all, of the responsiveness of *Selp* to TNF- α or LPS.

Trauma during surgical exposure of the cremaster muscle mobilizes P-selectin to the venular surface (17). Neutrophils rolled more slowly in trauma-stimulated venules of *Selp*^{K1/K1} mice, consistent with higher basal expression of P-selectin, whereas neutrophils rolled with similar velocities in venules of *Selp*^{K1/-} and WT mice (Fig. 4A). Intrascrotal injection of TNF- α increases synthesis of P- and E-selectin in WT mice (17, 30). We injected blocking anti-E-selectin mAb intravenously to isolate P-selectin-dependent rolling. Compared with velocities in trauma-stimulated venules, TNF- α reduced rolling velocities in WT mice, consistent with up-regulated synthesis of P-selectin. TNF- α did not alter velocities in *Selp*^{K1/-} mice (Fig. 4A). Injecting blocking anti-P-selectin mAb eliminated rolling.⁴ These results support increased basal expression but dampened inducible expression of P-selectin in knockin mice.

Similar numbers of neutrophils migrated into the peritoneum of WT, *Selp*^{K1/-}, and *Selp*^{K1/K1} mice 4 h after challenge with thioglycollate (Fig. 4B). Anti-P-selectin mAb reduced migration equivalently. Therefore, differences in basal or inducible expression of P-selectin did not alter neutrophil migration in this model, which may rely more on local macrophage release of chemokines like CXCL1 than of cytokines like TNF- α (31).

Both P- and E-selectin contribute to oxazolone-induced contact hypersensitivity in the ears of WT mice (17, 32–36). As observed previously (17), ear swelling in WT mice was reduced

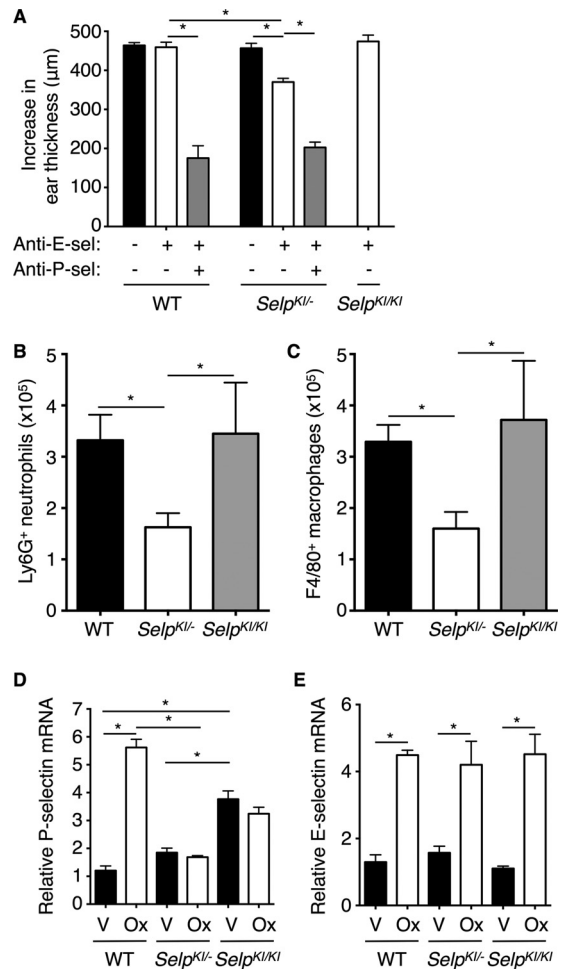


FIGURE 5. P-selectin-dependent contact hypersensitivity in *Selp*^{K1/K1} and *Selp*^{K1/-} mice. A, WT, *Selp*^{K1/K1}, or *Selp*^{K1/-} mice were sensitized with 2% oxazolone on the abdomen and paws. After 7 days, the mice were challenged with 1% oxazolone on the right ear and with vehicle only on the left ear. Immediately before the challenge, some mice were injected intravenously with anti-E-selectin mAb (*anti-E-sel*), anti-P-selectin mAb (*anti-P-sel*), or both anti-E-selectin and anti-P-selectin mAbs. Control mice received no treatment or were injected with saline, which yielded identical results. The net increase in ear thickness was measured 24 h after challenge ($n = 6\text{--}25$ mice/group). B and C, after measuring ear thickness, oxazolone-challenged ears of anti-E-selectin treated groups were digested for 3 h. The numbers of Ly6G⁺ or F4/80⁺ cells were quantified by flow cytometry ($n = 4\text{--}8$ mice/group). D and E, ears of WT, *Selp*^{K1/K1}, or *Selp*^{K1/-} mice were homogenized 8 h after challenge with vehicle (V) or oxazolone (Ox). P- or E-selectin mRNA was quantified and normalized to vehicle-treated ears of WT mice ($n = 4\text{--}10$ mice/group). Error bars are mean \pm S.E. *, $p < 0.05$.

by injecting anti-P-selectin and anti-E-selectin mAbs but not by anti-E-selectin mAb alone (Fig. 5A). Anti-E-selectin mAb alone decreased swelling in *Selp*^{K1/K1} mice but not in *Selp*^{K1/K1} mice. Fewer Ly6G-positive neutrophils or F4/80-positive monocytes/macrophages entered the inflamed ears of *Selp*^{K1/-} mice (Fig. 5, B and C). These data suggest that higher basal expression of P-selectin in *Selp*^{K1/K1} mice compensates for its blunted inducible expression. In the ears of WT mice, mRNA for P- and E-selectin peaks 8 h after oxazolone challenge (17). At this time point, we confirmed higher basal expression of P-selectin mRNA in the vehicle-challenged ears of *Selp*^{K1/K1} mice (Fig. 5D). Oxazolone-challenged ears up-regulated P-selectin mRNA only in WT mice (Fig. 5D), whereas they up-regulated E-selectin mRNA in all mice (Fig. 5E). In *SELP* transgenic

Human SELP Promoter Function in Mice

mice, P-selectin contributes much less to contact hypersensitivity, in part because of lower basal expression in dermal venules (17), as also observed in human skin (37). Therefore, substituting the *SELP* 1.4-kb promoter sequence confers human-like basal expression of P-selectin in most tissues but less so in skin.

Discussion

Remarkably, our results demonstrate that sequence variations limited to the 1.4-kb proximal promoter account for most of the differences in expression of the murine *Selp* and human *SELP* genes. Our data are derived from mice expressing a chimeric *Selp* that retains its entire genetic and epigenetic architecture except for the substituted proximal promoter from *SELP*. This approach permits comparative analysis of promoter function *in vivo* in a physiologically relevant environment. Previous studies of species-specific differences in gene expression used short promoter/enhancer sequences that drive reporter genes in transfected cells or in transgenic mice (38–44). Whether the identified regulatory elements function in the context of the native genes was not determined.

Our data for murine *Selp* and human *SELP* likely extend to the corresponding genes in other mammals. Genomic databases indicate that the canonical binding sites for NF- κ B and ATF-2 in the murine *Selp* promoter are conserved in *Selp* promoters of other mammals but not in *SELP* promoters of primates. The loss of these sites in primate promoters (19) probably explains the blunted up-regulation of P-selectin mRNA by TNF- α and other mediators. *Cis* elements outside of the 1.4-kb region may enable these mediators to further down-regulate mRNA in primates and may influence basal expression of P-selectin in skin and other tissues. Our results provide mechanistic insights into the differences in *Selp/SELP* expression that must be considered when extrapolating data from animal models to humans. Why regulatory sequences have diverged in primate *SELP* genes is an interesting issue for further study.

Author Contributions—Z. L., N. Z., B. S., and S. R. P. performed the research. Z. L., N. Z., J. F., and R. P. M. analyzed the data. Z. L., N. Z., and R. P. M. designed the research. N. Z. and R. P. M. wrote the paper with final approval from all authors.

References

1. Vestweber, D., and Blanks, J. E. (1999) Mechanisms that regulate the function of the selectins and their ligands. *Physiol. Rev.* **79**, 181–213
2. McEver, R. P., and Zhu, C. (2010) Rolling cell adhesion. *Annu. Rev. Cell Dev. Biol.* **26**, 363–396
3. McEver, R. P. (2015) Selectins: initiators of leucocyte adhesion and signaling at the vascular wall. *Cardiovasc. Res.* **107**, 331–339
4. Schweitzer, K. M., Dräger, A. M., van der Valk, P., Thijsen, S. F., Zevenbergen, A., Theijssmeijer, A. P., van der Schoot, C. E., and Langenhuijsen, M. M. (1996) Constitutive expression of E-selectin and vascular cell adhesion molecule-1 on endothelial cells of hematopoietic tissues. *Am. J. Pathol.* **148**, 165–175
5. Weninger, W., Ulfman, L. H., Cheng, G., Souchkova, N., Quackenbush, E. J., Lowe, J. B., and von Andrian, U. H. (2000) Specialized contributions by $\alpha(1,3)$ -fucosyltransferase-IV and FucT-VII during leukocyte rolling in dermal microvessels. *Immunity* **12**, 665–676
6. Chong, B. F., Murphy, J. E., Kupper, T. S., and Fuhlbrigge, R. C. (2004) E-selectin, thymus- and activation-regulated chemokine/CCL17, and in-

- tercellular adhesion molecule-1 are constitutively coexpressed in dermal microvessels: a foundation for a cutaneous immunosurveillance system. *J. Immunol.* **172**, 1575–1581
7. Collins, T., Read, M. A., Neish, A. S., Whitley, M. Z., Thanos, D., and Maniatis, T. (1995) Transcriptional regulation of endothelial cell adhesion molecules: NF- κ B and cytokine-inducible enhancers. *FASEB J.* **9**, 899–909
8. Tchernychev, B., Furie, B., and Furie, B. C. (2003) Peritoneal macrophages express both P-selectin and PSGL-1. *J. Cell Biol.* **163**, 1145–1155
9. Sanders, W. E., Wilson, R. W., Ballantyne, C. M., and Beaudet, A. L. (1992) Molecular cloning and analysis of *in vivo* expression of murine P-selectin. *Blood* **80**, 795–800
10. Weller, A., Isenmann, S., and Vestweber, D. (1992) Cloning of the mouse endothelial selectins: expression of both E- and P-selectin is inducible by tumor necrosis factor. *J. Biol. Chem.* **267**, 15176–15183
11. Auchampach, J. A., Oliver, M. G., Anderson, D. C., and Manning, A. M. (1994) Cloning, sequence comparison and *in vivo* expression of the gene encoding rat P-selectin. *Gene* **145**, 251–255
12. Bischoff, J., and Brasel, C. (1995) Regulation of P-selectin by tumor necrosis factor- α . *Biochem. Biophys. Res. Commun.* **210**, 174–180
13. Doré, M., and Sirois, J. (1996) Regulation of P-selectin expression by inflammatory mediators in canine jugular endothelial cells. *Vet. Pathol.* **33**, 662–671
14. Burns, S. A., DeGuzman, B. J., Newburger, J. W., Mayer, J. E., Jr., Neufeld, E. J., and Briscoe, D. M. (1995) P-selectin expression in myocardium of children undergoing cardiopulmonary bypass. *J. Thorac. Cardiovasc. Surg.* **110**, 924–933
15. Yao, L., Pan, J., Setiadi, H., Patel, K. D., and McEver, R. P. (1996) Interleukin 4 or oncostatin M induces a prolonged increase in P-selectin mRNA and protein in human endothelial cells. *J. Exp. Med.* **184**, 81–92
16. Yao, L., Setiadi, H., Xia, L., Laszik, Z., Taylor, F. B., and McEver, R. P. (1999) Divergent inducible expression of P-selectin and E-selectin in mice and primates. *Blood* **94**, 3820–3828
17. Liu, Z., Miner, J. J., Yago, T., Yao, L., Lupu, F., Xia, L., and McEver, R. P. (2010) Differential regulation of human and murine P-selectin expression and function *in vivo*. *J. Exp. Med.* **207**, 2975–2987
18. Pan, J., Xia, L., Yao, L., and McEver, R. P. (1998) Tumor necrosis factor- α or lipopolysaccharide-induced expression of the murine P-selectin gene in endothelial cells involves novel kB sites and a variant ATF/CRE element. *J. Biol. Chem.* **273**, 10068–10077
19. Pan, J., Xia, L., and McEver, R. P. (1998) Comparison of promoters for the murine and human P-selectin genes suggests species-specific and conserved mechanisms for transcriptional regulation in endothelial cells. *J. Biol. Chem.* **273**, 10058–10067
20. Pan, J., and McEver, R. P. (1993) Characterization of the promoter for the human P-selectin gene. *J. Biol. Chem.* **268**, 22600–22608
21. Pan, J., and McEver, R. P. (1995) Regulation of the human P-selectin promoter by Bcl-3 and specific homodimeric members of the NF- κ B/Rel family. *J. Biol. Chem.* **270**, 23077–23083
22. Bullard, D. C., Qin, L., Lorenzo, I., Quinlin, W. M., Doyle, N. A., Bosse, R., Vestweber, D., Doerschuk, C. M., and Beaudet, A. L. (1995) P-selectin/ICAM-1 double mutant mice: acute emigration of neutrophils into the peritoneum is completely absent but is normal into pulmonary alveoli. *J. Clin. Invest.* **95**, 1782–1788
23. Xia, L., Sperandio, M., Yago, T., McDaniel, J. M., Cummings, R. D., Pearson-White, S., Ley, K., and McEver, R. P. (2002) P-selectin glycoprotein ligand-1-deficient mice have impaired leukocyte tethering to E-selectin under flow. *J. Clin. Invest.* **109**, 939–950
24. Miner, J. J., Xia, L., Yago, T., Kappelmayer, J., Liu, Z., Klopocki, A. G., Shao, B., McDaniel, J. M., Setiadi, H., Schmidtke, D. W., and McEver, R. P. (2008) Separable requirements for cytoplasmic domain of PSGL-1 in leukocyte rolling and signaling under flow. *Blood* **112**, 2035–2045
25. Yago, T., Petrich, B. G., Zhang, N., Liu, Z., Shao, B., Ginsberg, M. H., and McEver, R. P. (2015) Blocking neutrophil integrin activation prevents ischemia-reperfusion injury. *J. Exp. Med.* **212**, 1267–1281
26. Kunkel, E. J., and Ley, K. (1996) Distinct phenotype of E-selectin-deficient mice: E-selectin is required for slow leukocyte rolling *in vivo*. *Circ. Res.* **79**, 1196–1204

27. Ramos, C. L., Kunkel, E. J., Lawrence, M. B., Jung, U., Vestweber, D., Bosse, R., McIntyre, K. W., Gillooly, K. M., Norton, C. R., Wolitzky, B. A., and Ley, K. (1997) Differential effect of E-selectin antibodies on neutrophil rolling and recruitment to inflammatory sites. *Blood* **89**, 3009–3018
28. Johnston, G. I., Bliss, G. A., Newman, P. J., and McEver, R. P. (1990) Structure of the human gene encoding granule membrane protein-140, a member of the selectin family of adhesion receptors for leukocytes. *J. Biol. Chem.* **265**, 21381–21385
29. Mayadas, T. N., Johnson, R. C., Rayburn, H., Hynes, R. O., and Wagner, D. D. (1993) Leukocyte rolling and extravasation are severely compromised in P selectin-deficient mice. *Cell* **74**, 541–554
30. Kunkel, E. J., Jung, U., and Ley, K. (1997) TNF- α induces selectin-mediated leukocyte rolling in mouse cremaster muscle arterioles. *Am. J. Physiol. Heart Circ. Physiol.* **272**, H1391–H1400
31. Cailhier, J. F., Partolina, M., Vuthoori, S., Wu, S., Ko, K., Watson, S., Savill, J., Hughes, J., and Lang, R. A. (2005) Conditional macrophage ablation demonstrates that resident macrophages initiate acute peritoneal inflammation. *J. Immunol.* **174**, 2336–2342
32. Staite, N. D., Justen, J. M., Sly, L. M., Beaudet, A. L., and Bullard, D. C. (1996) Inhibition of delayed-type contact hypersensitivity in mice deficient in both E-selectin and P-selectin. *Blood* **88**, 2973–2979
33. Catalina, M. D., Estess, P., and Siegelman, M. H. (1999) Selective requirements for leukocyte adhesion molecules in models of acute and chronic inflammation: participation of E- and P- but not L-selectin. *Blood* **93**, 580–589
34. Hwang, J. M., Yamanouchi, J., Santamaria, P., and Kubes, P. (2004) A critical temporal window for selectin-dependent CD4⁺ lymphocyte homing and initiation of late-phase inflammation in contact sensitivity. *J. Exp. Med.* **199**, 1223–1234
35. O'Leary, J. G., Goodarzi, M., Drayton, D. L., and von Andrian, U. H. (2006) T cell- and B cell-independent adaptive immunity mediated by natural killer cells. *Nat. Immunol.* **7**, 507–516
36. Labow, M. A., Norton, C. R., Rumberger, J. M., Lombard-Gillooly, K. M., Shuster, D. J., Hubbard, J., Bertko, R., Knaack, P. A., Terry, R. W., and Harbison, M. L. (1994) Characterization of E-selectin-deficient mice: demonstration of overlapping function of the endothelial selectins. *Immunology* **1**, 709–720
37. Silber, A., Newman, W., Reimann, K. A., Hendricks, E., Walsh, D., and Ringler, D. J. (1994) Kinetic expression of endothelial adhesion molecules and relationship to leukocyte recruitment in two cutaneous models of inflammation. *Lab. Invest.* **70**, 163–175
38. Rose, S. D., and MacDonald, R. J. (1997) Evolutionary silencing of the human elastase I gene (ELA1). *Hum. Mol. Genet.* **6**, 897–903
39. Thomas, G. P., Bourne, A., Eisman, J. A., and Gardiner, E. M. (2000) Species-divergent regulation of human and mouse osteocalcin genes by calcitropic hormones. *Exp. Cell Res.* **258**, 395–402
40. Spitsin, S. V., Koprowski, H., and Michaels, F. H. (1996) Characterization and functional analysis of the human inducible nitric oxide synthase gene promoter. *Mol. Med.* **2**, 226–235
41. Zhang, X., Laubach, V. E., Alley, E. W., Edwards, K. A., Sherman, P. A., Russell, S. W., and Murphy, W. J. (1996) Transcriptional basis for hyporesponsiveness of the human inducible nitric oxide synthase gene to lipopolysaccharide/interferon- γ . *J. Leukocyte Biol.* **59**, 575–585
42. Chu, S. C., Marks-Konczalik, J., Wu, H. P., Banks, T. C., and Moss, J. (1998) Analysis of the cytokine-stimulated human inducible nitric oxide synthase (iNOS) gene: characterization of differences between human and mouse iNOS promoters. *Biochem. Biophys. Res. Commun.* **248**, 871–878
43. Zhang, N., Weber, A., Li, B., Lyons, R., Contag, P. R., Purchio, A. F., and West, D. B. (2003) An inducible nitric oxide synthase-luciferase reporter system for *in vivo* testing of anti-inflammatory compounds in transgenic mice. *J. Immunol.* **170**, 6307–6319
44. Yu, Z., Xia, X., and Kone, B. C. (2005) Expression profile of a human inducible nitric oxide synthase promoter reporter in transgenic mice during endotoxemia. *Am. J. Physiol. Renal Physiol.* **288**, F214–220